On "resistance overpotential" caused by a potential drop along the ultrathin high aspect ratio gold nanowire electrodes in cyclic voltammetry.

I.S. Muratova[a,b], K.N. Mikhelson[b,1*], Yu. Ermolenko[b], A. Offenhäusser[a], Yu. Mourzina[a,*]

[a] Peter Grünberg Institute 8, Forschungszentrum Jülich GmbH and Jülich-Aachen Research Alliance - Fundamentals of Future Information Technology (JARA-FIT), 52428 Jülich, Germany

[b] Chemistry Institute, St. Petersburg State University, 26 Universitetskij Pr., 198504, St.Petersburg, Russia

*Corresponding author: Tel.:+49(0)2461612364. E-mail address: y.mourzina@fz-juelich.de (Dr. Yu. Mourzina); Tel.: +7 812 428 4062. E-mail: konst@km3241.spb.edu (Prof. K.N. Mikhelson)

Abstract

High aspect ratio ultrathin (d<10 nm) gold nanowires deposited on Si/SiO_2 substrate are used as working electrodes for measuring cyclic voltammograms (CVs) in aqueous solutions of ferrocene methanol and potassium hexacyanoferrate(III). The broadening of the peak separation as compared with that at a solid working electrode is explained as a result of the potential drop ("resistance overpotential") along nanowires and nanowire network. The change in the CV shape over a sequence of scans is ascribed to a gradual breakup of individual nanowires and the respective transition of the linear diffusion to hemispherical diffusion regularities.

[1] ISE member

Keywords

Ultrathin gold nanowires, resistance overpotential, potential drop.

1. Introduction

High aspect ratio ultrathin (d<10 nm) gold nanowires (NWs) prepared by a simple solution synthesis [1, 2] have attracted much attention for fundamental research and for applications as high-density interconnects [3] and chemiresistor sensors [4]. Using the Au NWs as an electrode network may increase the density and spatial resolution of electrochemical measurements and create a new type of a large-scale interface to biological matter [5]. A number of studies were devoted to the mechanism of conductivity [6-9], structural characterization and stability [10] of ultrathin Au NWs.

Promising sensing properties of devices based on ultrathin Au NWs were shown using a chemiresistor signal transduction principle, where the resistance of the device changes depending on the adsorption and charge on the NWs surface [4, 11]. Some studies demonstrated the modification of electrode materials with ultrathin metal nanowires matrix [12-14]. However, highly reproducible devices with regard to the number of NWs crossing the contact electrode gap and contact areas between the NWs and contact electrodes [6, 15] have not been practicable thus far. There are reports on low sensitivity, poor performance, and deviations in the cyclic voltammetry (CV) of low-dimensional electrodes [16, 17], where the electrode dimension approaches the mean free pathway of the electron in the metal, approx. 80 nm for Au, and an effect of inelastic surface scattering of electrons at wire surfaces starts to make a non-negligible contribution to the metal conductivity [18]. Additionally, synthesizing the NWs *in situ* on the substrate with pre-structured electrodes results in a growth of high density NPs on the surface of the metal contact electrodes and lines. This significantly increases the capacitive currents of the final devices and is unfavorable for

electrochemical sensors and interconnects applications. High current densities and Joule heating may additionally lead to breakup of NWs and electrical discontinuity in a nanowire network [19].

Size-dependent intrinsic properties of nanomaterials are advantageous for some applications, e.g., chemiresistive sensing [4, 20-27]. However, these properties cause crucial deviations in the NWs behavior as electrodes from that of classical metal electrodes. In the case of high aspect ratio nanowires, a potential drop may arise over the nanowire or/and the nanowire network. In other words, unlike classical electrodes, the NW electrodes may lack equipotentiality.

In this report we show, for the first time how the potential drop over ultrathin (d~3 nm) high aspect ratio gold nanowire electrode results in unusual cyclic voltammograms (CVs), decreased stability, and quasi-reversible behavior. This makes the interpretation of the data obtained with NW electrodes even more complex and we therefore present here only a qualitative discussion of the results.

2. Experimental

2.1. Materials

Oleylamine (OA), 70 %, toluene, ascorbic acid (AA), acetone, ethanol, propanol, sulfuric acid, ferrocene methanol, potassium hexacyanoferrate(III), potassium nitrate, gold(III) chloride trihydrate, and other chemicals of analytical grade employed in the synthesis and for electrochemical measurements were from Sigma-Aldrich. All solutions were prepared using deionized water (Millipore: Milli-Q Advantage A10 Ultrapure Water Purification System).

2.2. Synthesis of nanowires

The Si/SiO_2 (1 μm) substrates were diced 11x11 mm plates and cleaned in acetone, propanol, water, followed by 1:2 v/v of H_2O_2:H_2SO_4, and water. The gold nanowires were synthesized following the procedure described elsewhere [1, 28], with minor modifications. The cleaned Si/SiO_2 substrates were placed into the reaction vessel. 4 mg of $HAuCl_4 \cdot 3H_2O$ and 10 ml of toluene were stirred intensively, next, 80 μl of oleylamine was added, the mixture was sonicated for 10-15 seconds, and introduced into the reaction vessel covering the substrates. After that, the solution was heated from room temperature to about 100 °C (approximately the boiling temperature of toluene) and then refluxed at this temperature for 30-35 min until the color of the solution became light pink. The solution was then cooled down at 40 °C for 5 min. After that 16 mg of AA was added to the mixture, and the latter was aged for three hours, resulting in the formation of Au nanowires (NWs) on Si/SiO_2 substrate. The NWs were cleaned by washing in ethanol, water, and acetone.

2.3. Apparatus

Scanning electron microscopy (SEM) was carried out using a Zeiss Gemini 1550 instrument. The NWs network resistance was measured with Keithly semiconductor analyzer (model 4200 SCS). Cyclic voltammograms (CVs) were measured with potentiostat-galvanostat Autolab 302 (Ecochemie, The Netherlands).

The measurements were performed using the experimental setup shown in Figure 1.

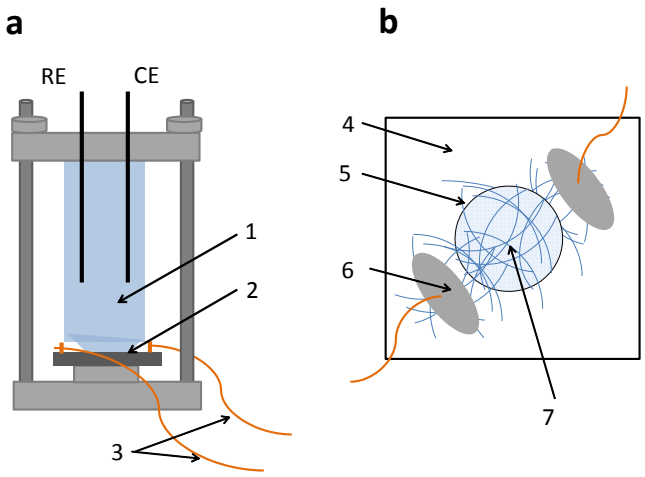

Fig. 1 a, b Scheme of the experimental setup. **a**: electrochemical cell, side view. **b**: substrate with NWs network in contact with solution, top view. 1 – solution, 2 – substrate with NWs network, 3 – contact wires, 4 – substrate, 5 – NWs network, 6 – contact pad (silver contact paste), 7 –working electrode in contact with solution

Electrical contact to the gold nanowire network deposited on a Si/SiO_2 substrate was made by attaching external metal wires using a silver contact paste. The diameter of the working electrode in the electrochemical cell was 6 mm, and the distance between silver paste electrical contact to the NWs and contact of the NWs to the electrolyte solution in the electrochemical cell was 2.5 mm. Part of the NWs randomly deposited on the substrate directly contacted the contact pads. The rest contacted these ones and each other forming the NW network.

For the measurements of the NWs network resistance, one of the two contact wires was kept at zero potential while the other one was either at +0.1 or at -0.1 V, and the electrode was in contact with air. On the contrary, for CV measurements the contact wires were short cut. CVs were measured in a three-electrode cell. A platinum coil was used as a counter electrode. The reference electrode was Ag/AgCl in 3 M KCl without KCl leakage in the frame of the experiment, which was achieved by using KONBO[a] as the liquid junction (3 M KCl, E^f = 0.210 V vs NHE, (DRIREF-450, WPI). The volume of the solution was 20 ml. The cell design ensured full coverage of the substrate and NWs with solution. Also, control was taken

that there were no air or argon (when removing oxygen) bubbles on the surface of the chip during the measurements. For a back-to-back comparison, a thin-film gold electrode Si 525 μm/SiO_2 1 μm/Ti 10 nm/Au 400 nm was also used as a working electrode. The experiments were performed at a single scan rate of 0.02 V s^{-1} because of the lack of the network stability, as discussed in the following section.

3. Results and Discussion

Figure 2 shows SEM image of the ultrathin Au NWs network grown on Si/SiO_2 substrate. One can see that the NWs form a continuous network on the surface of the substrate. Bright spots seen in SEM images are Au nanoparticles co-produced together with Au nanowires.

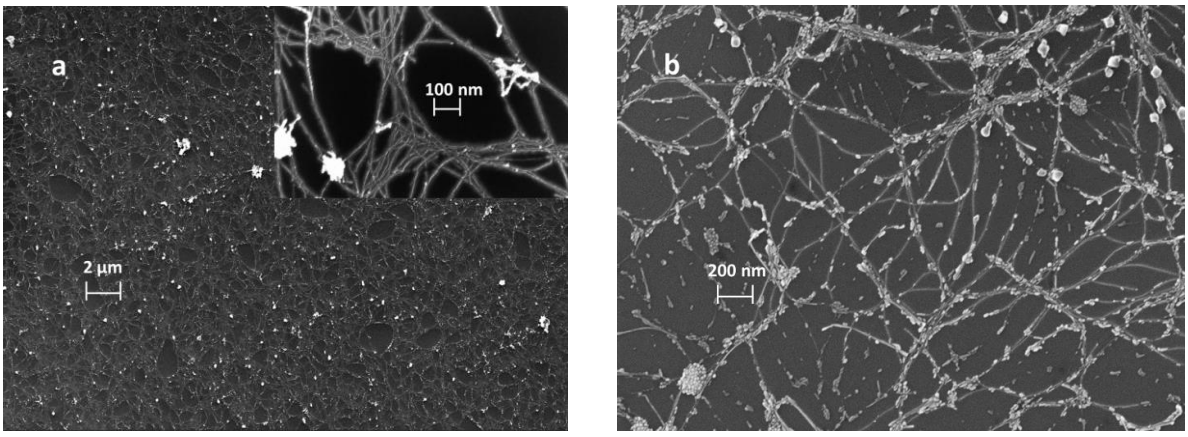

Fig. 2 a, b SEM images of a Si/SiO_2/Au NWs electrode: **a** - before and **b** - after cyclic voltammetry in 0.1 M sulfuric acid

The NWs network resistance was measured in contact with air. The results (see Figure 3) imply Ohmic behavior of the NWs network, and the resistance was rather high: $1.9 \cdot 10^6$ Ω.

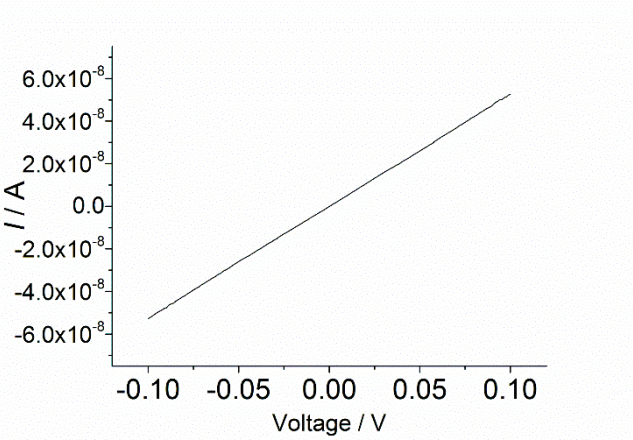

Fig. 3 Current-voltage plot of a NW network electrode in contact with air

Cycling in 0.1 M sulfuric acid is often used for the electrochemical cleaning and evaluation of the electroactive area of the working electrode [28]. The results obtained with the ultrathin Au NWs network grown on Si/SiO_2 substrate and with the thin-film gold electrode are presented in Figure 4. The electroactive area of the thin-film gold electrode [28] of 0.315±0.011 cm^2 was in agreement with the geometrical area of the working electrode in the electrochemical cell, while the electroactive area of the NWs exposed in the same electrochemical cells was 0.016±0.018 cm^2 (found using the first scans, n=4, and assuming that the surface activity of NWs is the same as that of bulk gold), i.e. about 20 times less. The reason for a poor reproducibility of the measurements in the case of ultrathin Au NWs networks is discussed below.

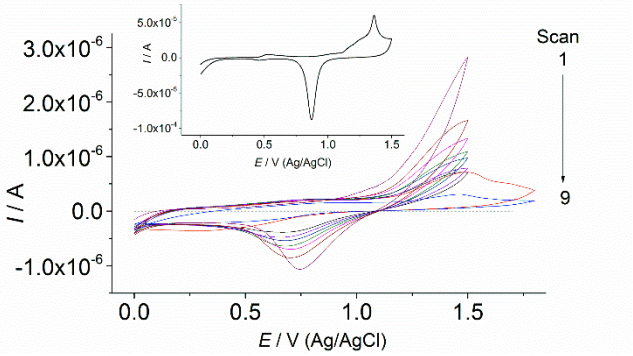

Fig. 4 CVs of a Si/SiO_2/Au NWs electrode in 0.1 M sulfuric acid, scans 1 to 9; a background (dashed) line corresponds to the Si/SiO_2. The inset shows CVs of a thin-film gold electrode Si/SiO_2 1 µm/Ti 10 nm/Au 400 nm, scan rate 0.02 V s^{-1}

Importantly, for the CV recording both wires contacting the NWs network were short cut, thus the contact pads were always equipotential. Therefore, it may appear that when a CV is recorded, all the NWs in the NWs network are also at the same potential. If this would be true, the gold NWs network electrode would produce a CV of the same shape as a thin-film gold electrode. However, the results presented in Figure 4 indicate different. The CVs obtained with the NWs network electrode are rather smooth when compared with those for the thin film gold electrode. Also, the peak separation for the thin film electrode was 0.4 V while that for the NWs network electrode was 0.74 V in initial scans and increased to 1.18 V in the last scan.

We believe that this difference can be explained as follows. Although the contact wires in CV measurements were short cut, the NWs in the NWs network in the electrochemical cell shown in Figure 1a are at the same potential only in the absence of electrochemical processes at such an electrode. If some electrochemical process takes place at some point in the NWs network then the respective oxidation or reduction current flows along NWs to the contact pads, and therefore an *IR* drop arises between this particular point in the NWs network and the contact pad. Due to a large resistance of the NWs network this *IR* drop is significant, and alters the shape of the CVs.

It was shown that the resistivity of the gold NW network is essentially higher than that of the bulk metal (2.44×10^{-8} Ω m) and of thin films, and could be approximated as several hundreds to 1000 Ω·nm [3, 4, 29]. According to our data shown in Figure 3, the resistance of the NWs network studied here was about 2 MΩ suggesting *IR* drop of 2 V for a current of 1 μA. The actual *IR* drop must be smaller because the parts of the NWs network located closer to the contact pads contribute to the overall current more than those located in the central part of the network. However, the occurrence of the *IR* drop over the NWs network electrode might explain an increasing separation of the redox peaks and peaks shift with the scan number, while the NWs become even thinner and more resistive in each subsequent scan.

This potential drop might be considered by a resistance overpotential parameter which to some extent is similar to the Ohmic potential drop between the reference and working electrodes in electrochemical cells due to the uncompensated solution resistance [30, 31] (e.g., in low electrolyte concentrations). G. Booman and coworkers published a series of papers on *IR* drop in three-electrode cell configurations, and on compensation thereof using a potentiostat with positive feedback [32]. More recently it was shown that the effect of the uncompensated resistance can be quantitatively described for a uniform distribution of the potential over the surface of the working electrode [33]. However, our case appears significantly different because the uncompensated nanowire resistance in the present study resulted in the gradient of the potential along the NW. Consequently, it is difficult to introduce a defined value of this parameter over the length of the nanowire network electrode, because it depends on the distance from the contact point to the NWs from the external circuitry and on a percolation pathway [15], so that various points on the NW network working electrode have different values of the potential against the reference electrode. Thus, the electrochemical process starts closer to the contact point to the NWs from the external circuitry and continues along the length of the NWs with increasing applied potential, and is finally canceled on the NW segments, where the potential is not enough for the reaction to proceed: due to the potential drop along the length of the NWs network. Therefore, we assume that the electrochemical processes shown in Figures 4 and 5 proceed primarily on the NW surfaces close to the contact point, but hardly in the middle of the working electrode. Application of higher potentials finally resulted in breaking the wire connections, see Figure 2b and Figure 4 (scans 8, 9), probably due to oxidation and Joule heating. Partial destruction of the NWs network after cycling in sulfuric acid is confirmed also by SEM images, compare Figures 2a and 2b. Additionally, electrodes with longer distances between the contact point to the NWs and the electrolyte (5 mm) show no electrochemical response since even higher voltages should be applied to drive an electrochemical reaction.

Therefore, we would like to emphasize here that a more detailed study, e.g., with the variation of scan rate or concentration of the redox probes for quantitative interpretation of the data is hardly possible in this case. Furthermore, actual magnitudes are given rather for qualitative estimation, because the networks are unstable even in a narrow potential window and are intrinsically not reproducible.

In principle, the surface activity of the nanowires may be lower than that of bulk gold. Also, the extent of the overlapping of the diffusional layers may be different in different parts of the NW network. These factors may additionally contribute to the broadening of the peak separation. The decrease of the current with the scan number also implies gradual dissolution of NWs in the sulfuric acid.

The results are further supported by CV measurements with ferrocene methanol and hexacyanoferrate, Figures 5a and 5b, respectively. Before recording the CVs, the electrodes were pretreated for 6 s at the cathodic vertex potential: -0.2 V.

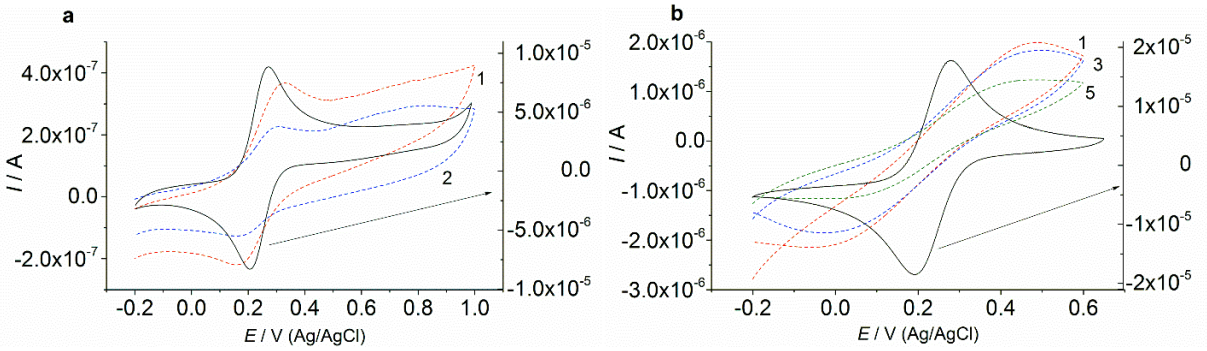

Fig. 5 a, b Cyclic voltammogramms of: **a** – ferrocenemethanol, $5 \cdot 10^{-5}$ M, scans 1 and 2; **b** - hexacyanoferrate(III), $1 \cdot 10^{-3}$ M, scans 1,3,5, Au NWs on Si/SiO_2. Black solid lines with a right-hand Y-scale in **a**, **b** are CVs on a Si/SiO_2/Au thin-film gold electrode of $5 \cdot 10^{-4}$ M ferrocenemethanol and $1 \cdot 10^{-3}$ M hexacyanoferrate(III), respectively. Background electrolyte: 0.1 M KNO_3, scan rate rate 0.02 V s^{-1}

Voltammetric curves for the NW electrodes generally appeared less reversible than for the thin-film gold electrodes which are not affected by the electrical resistance of a metal film. The peak separation was about 64 mV ($E_{p,c}$= 0.211 V, $E_{p,a}$= 0.275 V) for ferrocene methanol

and 105 mV ($E_{p,c}$= 0.196 V, $E_{p,a}$= 0.301 V) for hexacyanoferrate(III) on the thin-film gold electrodes, see Figure 5 (black solid lines). Similar parameters were found earlier for the gold nanostructures grown on the gold thin-film electrodes *in situ* by the same methods of synthesis and cleaning proving that there was no inhibition of the electron transfer due to the surface impurities [28]. However, the peak separations for these redox couples on the Au NWs network electrode increase to 152 mV ($E_{p,c}$= 0.173 V, $E_{p,a}$= 0.325 V) and 485 mV ($E_{p,c}$= -0.007 V, $E_{p,a}$= 0.478 V) for ferrocene methanol and hexacyanoferrate respectively, due to the potential drop along the Au NWs network. Because of this drop, actual potential values (modulus) along a NW are lower than the applied potential value. Accordingly, the cathodic and anodic peak potentials are shifted to the negative and positive values, respectively. The potential drop is distributed over the whole NW network, and the broadening of the CVs is an integral effect, which can be formalized in terms of an effective resistance. The concentration of hexacyanoferrate solution was higher than that of ferrocene methanol, and the respective peak currents were also higher both for the thin-film gold electrode and for Au NWs electrode. Therefore much larger peak separation for Au NWs electrode in hexacyanoferrate solution is qualitatively in line with our interpretation. However, the current typically decreases with scan number, see Figures 5a, 5b, which confirms the breakup of the NWs connections (also seen in Figure 2b after cycling in 0.1 M sulfuric acid), probably, because of easy oxidation and Joule heating caused by the high resistivity [19, 34, 35]. We observed consequent decrease of the current with each scan number even in a narrow potential range, which demonstrates instability of the working electrode due to internal resistance and makes quantitative interpretations essentially meaningless. This instability makes the studies at various scan rates virtually useless, especially at lower scan rates because longer measurements and currents passed through the NWs may additionally contribute to destroying the NW s and/or NWs connections.

A larger peak separation, and a larger increase in the peak separation for a hexacyanoferrate (II/III) couple might be additionally due to the lower electron transfer rate (k^0=0.03 cm/s [36, 37]) than that for ferrocenemethanol (k^0=0.2 cm/s [36, 38]) because of the bridge transition state pathway in the electron transfer in the anion redox process and complex reorganization, where the rate of the bridge-assisted electron transfer is higher than that of the direct electron transfer. However, this three-body problem in electron transfer is not within the scope of the present work and may require further investigations [39-41].

The change in the shape of the CVs to less-defined peak currents may be explained as follows: initially, the NW network is dense and the diffusion layers around the individual NWs overlap. Overlapping of diffusional layers may lead to the formation of voltammetric peaks on CVs. However, with the increased number of scans, some NW electrodes connections break. Due to multiple percolation pathways in the NW network, a breakup of an individual wire connection does not totally exclude this wire from the electrically conducting network. But because of these breaks the amount of active NW electrodes decreases and the distance between them increases. Respectively, the initial linear diffusion is gradually replaced with a hemispherical diffusion [42].

These results are consistent with some earlier reports on low-dimensional electrodes. Tyagi et al. [16] supposed that CV curves and low sensitivity of a Au NW 30 nm in width and 200 nm in thickness prepared by lithography were influenced by a voltage drop along the NWs due to a difference in electrical resistance, which might be one order of magnitude larger for the 30 nm wide NWs as compared to the wider wires with a 200 nm diameter. The loss of details in CV curves (i.e. hydrogen adsorption and desorption, platinum oxide reduction peaks) was also reported for the Pt thin film electrodes of approx. 5 and 13 nm in thickness. The effect was ascribed to the high film resistance and significant potential gradients across the electrode, with only part of the electrode being at the applied potential, and the other part being at lower or higher potentials [17]. High resistance of the film also accounted for the displacement of

the CV of the film electrode relative to the solid electrode along the potential axis. A quasi-reversible behavior of a nanoneedle of multiwall carbon nanotube 30 nm in diameter, in $Fe(CN)_6^{3-}$ $E_{p,c}$= 0.213 V, $E_{p,a}$= 0.380 V, and ΔE=0.167 was also assumed to be due to the intrinsic electronic properties of MWCNT [43]. Thus, evaluating the functionality of nanomaterials under specific conditions is crucial for their integration as functional components in miniaturized devices.

The experimental results described here support the opinion that the finite size effect [22] complicates the employment of ultrathin NWs network over distance of several mm, and without high-resolution techniques to prepare contact lines and insulation of NW electrodes/electrochemical NW devices. Although ultrathin NW electrodes with lengths in the nm [44] can be used, the advantage of high aspect ratio network is not utilized in such applications.

Further studies may be required to explain other features of the CVs of the nanowires. In particular, peak broadening and the distribution of redox potential values might be influenced by different weights of the exposed plane gold surfaces, defects and edges of the nanostructures [45], and some dispersion in the nanostructure size distribution. Further factors which may influence the voltammograms are interactions of the electrical double layers of the nanowires and microelectrode-type behavior.

4. Conclusions

Our results demonstrate that ultrathin NW networks have electrical connectivity over distances within the mm range. However, the intrinsic high resistivity of the nanosized metals due to the diffusive scattering of electrons at the surface, as well as the geometry of the NWs *per se*, causes a potential drop along ultrathin gold nanowires. The respective resistance overpotential should be taken into consideration when using individual nanowires and their

network on non-conductive substrates for electrochemical systems. Furthermore, the low stability and short lifetime of individual nanowires are displayed in the change of the shape of the CVs over a sequence of scans.

Greater knowledge on the electrochemical properties of ultrathin gold NWs is required for future development in electrochemical sensor applications.

Conflict of interest

The authors declare no conflict of interest.

Acknowledgements

Ms. Hannah Freyer is gratefully acknowledged for the improving of the English of the paper. Dr. G. Panaitov is gratefully acknowledged for helpful discussions. Financial support from the Russian Foundation for Basic Research (RFBR) grant 14-03-01079 for studies on the nanostructure synthesis, and St. Petersburg State University grant 12.38.218.2015 for the electrochemical studies is gratefully acknowledged.

References

[1] Halder A, Ravishankar N (2007) Ultrafine Single-Crystalline Gold Nanowire Arrays by Oriented Attachment. Adv. Mater. 19 : 1854-1858

[2] Kisner A, Heggen M, Fernández E, Lenk S, Mayer D, Simon U, Offenhäusser A, Mourzina Y (2011) The Role of Oxidative Etching in the Synthesis of Ultrathin Single Crystalline Au Nanowires. Chemistry – A Europ. J. 17 : 9503-9507

[3] Roy A, Pandey T, Ravishankar N, Singh AK (2013) Single crystalline ultrathin gold nanowires: Promising nanoscale interconnects. AIP Advances 3 : 032131-1-032131-7

[4] Kisner A, Heggen M, Mayer D, Simon U, Offenhäusser A, Mourzina Y (2014) Probing the effect of surface chemistry on the electrical properties of ultrathin gold nanowire sensors. Nanoscale 6 : 5146-5155

[5] Liu J, Fu TM, Cheng Z, Hong G, Zhou T, Jin L, Duvvuri M, Jiang Z, Kruskal P, Xie C, Suo Z, Fang Y, Lieber CM (2015) Syringe-injectable electronics. Nat. Nanotech. 10 : 629-636 doi:10.1038/nnano.2015.115

[6] Pud S, Kisner A, Heggen M, Belaineh D, Temirov R, Simon U, Offenhäusser A, Mourzina Y, Vitusevich S (2013) Features of Transport in Ultrathin Gold Nanowire Structures. Small 9 : 846-852

[7] Guerin H, Yoshihira M, Kura H, Ogawa T, Sato T, Maki H (2012) Coulomb blockade phenomenon in ultra-thin gold nanowires. J. Appl. Phys. 111 : 054304-1-054304-4

[8] Loubat A, Escoffier W, Lacroix LM, Viau G, Tan R, Carrey J, Warot-Fonrose B, Raquet B (2013) Cotunneling transport in ultra-narrow gold nanowire bundles. Nano Res. 6 : 644-651

[9] Chandni U, Kundu P, Singh AK, Ravishankar N, Ghosh A (2011) Insulating State and Breakdown of Fermi Liquid Description in Molecular-Scale Single-Crystalline Wires of Gold. ACS Nano 5 : 8398–8403

[10] Lacroix LM, Arenal R, Viau G (2014) Dynamic HAADF-STEM Observation of a Single-Atom Chain as the Transient State of Gold Ultrathin Nanowire Breakdown. J. Am. Chem. Soc. 136 : 13075–13077

[11] Roy A, Pandey T, Ravishankar N, Singh AK (2014) Semiconductor-like Sensitivity in Metallic Ultrathin Gold Nanowire-Based Sensors. J. Phys. Chem. C 118 : 18676–18682

[12] Koposova E, Kisner A, Shumilova G, Ermolenko Y, Offenhäusser A, Mourzina Y (2013) Oleylamine-Stabilized Gold Nanostructures for Bioelectronic Assembly. Direct Electrochemistry of cytochrome *c*. J. Phys. Chem. C 117 : 13944–13951

[13] Xia BY, Wu HB, Yan Y, Lou XW, Wang X (2013) Ultrathin and Ultralong Single-Crystal Platinum Nanowire Assemblies with Highly Stable Electrocatalytic Activity. J. Am. Chem. Soc. 135 : 9480–9485

[14] Koposova E, Liu X, Kisner A, Ermolenko Y, Shumilova G, Offenhäusser A, Mourzina Y (2014) Bioelectrochemical systems with oleylamine-stabilized gold nanostructures and horseradish peroxidase for hydrogen peroxide sensor. Biosens. Bioelectron 57 : 54-58

[15] Langley DP, Lagrange M, Giusti G, Jiménez C, Bréchet Y, Nguyen ND, Bellet D (2014) Metallic nanowire networks: effects of thermal annealing on electrical resistance. Nanoscale 6 : 13535-13543

[16] Tyagi P, Postetter D, Saragnese DL, Randall CL, Mirski MA, Gracias DH (2009) Patternable Nanowire Sensors for Electrochemical Recording of Dopamine. Anal. Chem. 81 : 9979-9984

[17] Dickinson T, Sutton PR (1974) The study of adsorption by measurement of electrode resistance. Electrochim. Acta 19 : 427-435

[18] Fuchs K (1938) The conductivity of thin metallic films according to the electron theory of metals. Proc. Cambridge Philos. Soc. 34 : 100-108

[19] Khaligh HH, Goldthorpe IA (2013) Failure of silver nanowire transparent electrodes under current flow. Nanoscale Res. Lett. 8 : 235-231

[20] Duan BK, Zhang J, Bohn PW (2012) Conductance-Based Chemical Sensing in Metallic Nanowires and Metal-Semiconductor Nanostructures. Anal. Chem. 84 : 2-8

[21] Liu Z, Searson PC (2006) Single nanoporous gold nanowire sensor. J. Phys. Chem. B 110 : 4318-4322

[22] Hung D, Liu Z, Shah N, Hao Y, Searson PC (2007) Finite Size Effects in Ordered Macroporous Electrodes Fabricated by Electrodeposition into Colloidal Crystal Templates. J. Phys. Chem. C 111 : 3308-3313

[23] He H, Tao N (2002) Interactions of Molecules with metallic quantum wires. Adv. Mater.14 : 161-164

[24] Li SJ, Du JM, Chen J, Mao NN, Zhang MJ, Pang H (2014) Electrodeposition of cobalt oxide nanoparticles on reduced graphene oxide: a two-dimensional hybrid for enzyme-free glucose sensing, J. Solid State Electrochem. 18 : 1049–1056

[25] Radhakrishnan S, Siju CR, Mahanta D, Patil S, Madras G (2009) Conducting polyaniline–nano-TiO_2 composites for smart corrosion resistant coatings. Electrochim. Acta 54 : 1249-1254

[26] Wang Q, Zhang Y, Ye W, Wang C (2016) $Ni(OH)_2$/MoSx nanocomposite electrodeposited on a flexible CNT/PI membrane as an electrochemical glucose sensor: the synergistic effect of $Ni(OH)_2$ and MoSx. J. Solid State Electrochem. 20 : 133-142

[27] Scanlon MD, Peljo P, Mendez MA, Smirnov E, Girault HH (2015) Charging and discharging at the nanoscale: Fermi level equilibration of metallic nanoparticles. Chem. Sci. 6 : 2705-2720

[28] Nikolaev K, Ermakov S, Ermolenko Y, Averyaskina E, Offenhäusser A, Mourzina Y (2015) A novel bioelectrochemical interface based on in situ synthesis of gold nanostructures on electrode surfaces and surface activation by Meerwein's salt. A bioelectrochemical sensor for glucose determination. Bioelectrochem. 105 : 34-43

[29] Song JH, Wu Y, Messer B, Kind P, Yang P (2001) Metal Nanowire Formation Using $Mo3Se_3^-$ as Reducing and Sacrificing Templates, J. Am. Chem. Soc. 123 : 10397-10398

[30] Bowden FP, Agar JN (1938) General and physical chemistry. 5: Irreversible electrode process, Ann. Rep. Chem. Soc. 35 : 90-113

[31] Scholz F (ed) (2002) Electroanalytical methods. Springer, Berlin, Heidelberg

[32] Brown ER, Smith DE, Booman GL (1968) A Study of Operational Amplifier Potentiostats Employing Positive Feedback for IR Compensation 1. Theoretical Analysis of Stability and Bandpass Characteristics. Anal. Chem. 40 : 1411-1423

[33] Feldberg SW (2008) Effect of uncompensated resistance on the cyclic voltammetric response of an electrochemically reversible surface-attached redox couple: Uniform current and potential across the electrode surface. J. Electroanal. Chem. 624 : 45-51

[34] Fangohr H, Chernyshenko DS, Franchin M, Fischbacher T, Meier G (2011) Joule heating in nanowires. Phys. Rev. B 84 : 054437-1-054437-12

[35] Popp E (2010) Energy dissipation and transport in nanoscale devices, Nano Res 3 : 147-169

[36] Cannes C, Kanoufi F, Bard AJ (2003) Cyclic voltammetry and scanning electrochemical microscopy of ferrocenemethanol at monolayer and bilayer-modified gold electrodes. J. Electroanal. Chem. 547 : 83-91

[37] Marecek V, Samec Z, Weber J (1978) The dependence of the electrochemical charge-transfer coefficient on the electrode potential. Study of the $Fe(CN)^{3-}_{6}/Fe(CN)^{4-}_{6}$ redox reaction on polycrystalline Au electrode in KF solutions. J. Electroanal. Chem. 94 : 169-185

[38] Bourdillon C, Demaille C, Moiroux J, Saveant JM (1995) Catalysis and mass transport in spatially ordered enzyme assemblies on electrodes, J. Am. Chem. Soc. 117 : 11499-11506

[39] Swaddle TW (2005) Homogeneous versus Heterogeneous Self-Exchange Electron Transfer Reactions of Metal Complexes: Insights from Pressure Effects. Chem. Rev. 105 : 2573-2608

[40] Dogonadze RR, Ulstrup J, Kharkats YI (1972) A theory of electrode reactions through bridge transition states; bridges with a discrete electronic spectrum. J. Electroanal. Chem. 39 : 47-61

[41] Krulic D, Fatouros N, Khoshtariya DE (1998) Kinetic data for the hexacyanoferrate (II)/(III) couple on platinum electrode in various chlorides of monovalent cations. J. Chim. Phys. 95 : 497-512

[42] Scharifker BR (1988) Diffusion to ansembles of microelectrodes. J Electroanal. Chem 240 : 61-76

[43] Boo H, Jeong RA, Park S, Kim KS, An KH, Lee YH, Han JH, Kim HC, Chung TD (2006) Electrochemical Nanoneedle Biosensor Based on Multiwall Carbon Nanotube. Anal. Chem. 78 : 617-620

[44] Li Y, Wu Q, Jiao S, Xu C, Wang L (2013) Single Pt Nanowire Electrode: Preparation, Electrochemistry, and Electrocatalysis. Anal. Chem. 85 : 4135–4140

[45] Kleijn SEF, Lai SCS, Koper MTM, Unwin PR (2014) Electrochemistry of nanoparticles, Angew. Chem. Int. Ed. 53 : 3558-3586